We are IntechOpen,
the world's leading publisher of
Open Access books
Built by scientists, for scientists

4,800
Open access books available

122,000
International authors and editors

135M
Downloads

Our authors are among the

154
Countries delivered to

TOP 1%
most cited scientists

12.2%
Contributors from top 500 universities

BOOK
CITATION
INDEX
CLARIVATE ANALYTICS
INDEXED

WEB OF SCIENCE™

Selection of our books indexed in the Book Citation Index
in Web of Science™ Core Collection (BKCI)

Interested in publishing with us?
Contact book.department@intechopen.com

Numbers displayed above are based on latest data collected.
For more information visit www.intechopen.com

Computational Fluid Dynamics (CFD) Modeling of Photochemical Reactors

Masroor Mohajerani, Mehrab Mehrvar and Farhad Ein-Mozaffari
Department of Chemical Engineering, Ryerson University, Toronto, Ontario
Canada

1. Introduction

Advanced oxidation processes (AOPs) play an important role in the degradation or the production of a wide range of organic materials. Many organic compounds such as pharmaceuticals, dyes, herbicides, and pesticides have been subjected to degradation and remediation purposes in water and wastewater treatment systems using AOPs. Some of the organic compounds such as drugs, vitamins, or fragrances could be also produced by oxidation processes.

As the standard of living increases, many chemicals such as pharmaceuticals, pesticides, herbicides, and dyes are extensively consumed. Each of these products may cause health issues by their accumulation in aquatic environment. Pharmaceuticals such as antibiotics are partially metabolized and excreted by humans and animals. Improper disposal, dumping, and accidental discharge of drugs lead to the increase of the concentration of compounds such as analgesics, antibiotics, steroids, and hormones in aquatic environment, which cause environmental and health problems. Residual pesticides and herbicides originate from the direct pollutant in production plant, disposal of empty containers, equipment washing, and surface runoff. High levels of these compounds are toxic, mutagenic, carcinogenic, and tumorigenic. Some other wastes such as landfill leachate are subjected to advanced treatment methods. Old landfill leachates (>10 years) are nonbiodegradable in nature due to the existence of organic compounds with high molecular weights. Although the composition of landfill leachates varies widely with respect to the age of the landfill, type of wastes, and climate conditions, they can be categorized into four groups of dissolved organic matter, inorganic macro components, heavy materials, and xenobiotic organic substances. Another type of toxic chemicals which cannot be removed using conventional treatment methods is endocrine disrupting compounds (EDCs). EDCs, especially the steroidal hormones, are well recognized exogenous agents that interfere with the synthesis, action, and/or elimination of natural hormones in the body. Conventional processes are not effective in destruction of these types of organic compounds; therefore, powerful advanced treatment processes are required in order to mineralize them. There are several options for choosing an oxidation process: wet air oxidation, supercritical water oxidation, incineration, and AOPs.

AOPs have been promising in the treatment of contaminated soils and waters. The AOPs could be employed to fully or partially oxidize organic pollutants usually using a combination of different oxidants. In contrary to the conventional physical and chemical treatment processes, AOPs do not transfer pollutants from one phase to another, i.e., organic

pollutants are completely destroyed. Most AOPs are able to generate hydroxyl radicals. These hydroxyl radicals are active and powerful, capable of reacting with almost all types of organics, including non-biodegradable and recalcitrant compounds. These oxidizing hydroxyl radicals are initiated by photolysis, photocatalysis, sonolysis, radiolysis, and other AOPs alone or in combination in the presence of some reagents such as hydrogen peroxide (H_2O_2), ozone, and homogeneous or heterogeneous catalysts. Hydroxyl radicals are extremely powerful, short-lived oxidizing agent, and non-selective in nature and could react with a wide range of organic chemicals with reaction constant of several orders of magnitude higher than the reaction with molecular ozone under the same conditions. AOPs are used to convert toxic, non-biodegradable, inhibitory, and recalcitrant pollutants into simpler and less harmful intermediates, so they could be treated subsequently in biological processes. Due to the high operating and capital costs of AOPs, the complete mineralization of organic compounds using AOPs is practically impossible; therefore they are mainly combined with other processes such as biological systems to be cost-effective. With sufficient contact time and proper operating conditions and design, the mineralization efficiency of the AOPs is maximized by optimization of the processes in such a way that the total costs of the processes are minimized while the removal rates of organic pollutants are maximized.

Since conducting experiments is time-consuming and expensive or sometimes impossible to do, the modeling of the photoreactors is necessary. Computational fluid dynamics (CFD) is one of the numerical methods to solve and analyze the transport equations. CFD has been used recently in order to find the velocity, radiation intensity, pollutant concentration distribution inside the photoreacotrs (Mohajerani *et al.*, 2010,2011; Qi *et al.*, 2011; Duran *et al.*, 2011a,b, 2010; Vincent *et al.*, 2011; Denny *et al.*, 2009,2010; Elyasi and Taghipour, 2006; Taghipour and Mohseni, 2005; Mohseni and Taghipour, 2004). In this chapter, the velocity distribution in ten different configurations of single lamp and multi-lamp photoreactors in both laminar and turbulent regimes are provided. Moreover, the light intensity distribution inside the photoreactors is also presented.

2. Photoreactor design

The design and analysis of photochemical reactors have attracted researchers' interests for the past four decades. The main advantages of the photoreactors over the conventional thermal excitation reactors are their selectivity and low operating temperature. In spite of these advantages, photoreactors are not widely used in industrial scale. The use of a photoreactor results in higher product costs; therefore, the photochemical process is used when there are no other available feasible alternative conventional (thermal or catalytic) processes. Some other disadvantages such as size limitations, design and construction difficulties, and fouling on lamp walls have restricted industrial applications of these types of reactors.

Radiation field is the main characteristic of photoreactors determining the kinetics and the photoreactor performance. The photochemical reaction rate is proportional to the local volumetric rate of energy absorption (LVREA), an important parameter playing a crucial role in the photoreactor design. The LVREA depends on the radiation field presents within the photoreactor. The LVREA is a complex function of the lamp intensity, the concentration of absorbing species, the geometrical characteristics of the photoreactor system, and some other physicochemical properties. The light attenuation caused by the absorbing species

makes the LVREA non-uniform. A Photochemical reactor design requires the solution of momentum, energy, and mass balances. The expression for the conservation of momentum is similar to that of the conventional reactor. It is believed that light irradiation does not affect the photochemically reactive fluid flow. The mass balance or continuity equations for each compound in the system should be solved simultaneously to find the concentration profile of each compound inside the photoreactor.

The mass and energy conservation equations are directly related to the light irradiation. The energy balance can be divided into two parts: thermal and radiant energy balances. Although for isothermal photochemical reactions, thermal balances are negligible, a complete equation of change for energy balance is required for exothermic and endothermic reactions. The first step in the LVREA evaluation is to state a radiant energy balance at steady state condition in a homogeneous system. A radiation source model is also needed to be considered. Different source models have been developed during the past years to describe the radiant energy field and to calculate the LVREA.

Gaertner and Kent (1958) were among the first group that modeled photochemical reactions. They studied the photolysis of aqueous uranyl oxalate in an annular tubular reactor. The results of their experiments were correlated with a remarkable accuracy by assuming that the rate of photolysis is proportional to the residence time multiplied by the intensity of radiation at a particular radial position. They also proposed a mathematical model without considering the reactant concentration. Therefore, their model was applicable when the conversion was small (less than 12%). The effect of diffusion was also neglected in their model.

The modeling of radiation field is classified into two categories: incidence and emission models. In the former approach, a specific radiation distribution exists in the photoreactor, while in the latter approach, the photon emission rate is employed to derive an incidence model. Although incidence models are mathematically simple to implement, there is no way of using this approach without experimentally adjustable parameters. Therefore, this approach cannot be employed as a reasonable systematic method to design photoreactors. Different incidence models have been developed and used for photoreactor modeling including radial incidence model (Gaertner and Kent, 1958; Schechter and Wissler, 1960; Cassano and Smith, 1966, 1967; Cassano *et al.*, 1968; Matsuura and Smith, 1970b, 1971; Santeralli and Smith, 1974; Dolan *et al.*, 1965; Jacob and Dranoff 1969; Williams and Ragonese, 1970), partially diffuse model (Matsuura and Smith, 1970a), and diffuse incidence model (Jacob and Dranoff, 1969; Williams, 1978; Matsuura *et al.*, 1969; Matsuura and Smith, 1970c; Harada *et al.*, 1971; Roger and Villermaux, 1983).

In emission model, a lamp is considered as an emitting line, a surface, or a volume source. Different emission models have been developed including line source with parallel plane emission model (Harris and Dranoff, 1965), line source with spherical emission model (Jacob and Dranoff, 1966, 1968, 1970; Jain *et al.*, 1971; Dworking and Dranoff, 1978; Magelli and Santarelli, 1978; Pasquali and Santarelli, 1978), and line source with diffuse emission model (Akehata and Shirai, 1972). Line and surface models are classified into specular and diffuse emission models. In specular emission, the magnitude of the light intensity vector is not a function of the emission angle. Photoreactors equipped with mercury arc and neon lamps belong to this class, while fluorescent lamps, in which the magnitude of the light intensity vectors depend on the angle of the emission, fall into the diffuse emission. There are some great reviews in which developed models describing the light distribution in photoreactors are presented in details in the open literature (Alfano *et al.*, 1986a,b; Cassano *et al.*, 1995; Alfano and Cassano, 2009).

Photoreactors are generally grouped into homogeneous and heterogeneous classes. Homogeneous reactors operate in a single phase, gas or liquid, in air and water purification systems. In heterogeneous photoreactors, a photocatalyst is added to the system in order to increase the process efficiency. Heterogeneous photoreactors are subcategorized into attached (immobilized) or suspended (slurry) modes. Most of the early photoreactors have employed a titanium dioxide (TiO_2) suspension because it offers a high surface area for the reactions and almost no mass transfer limitation exists in the system. In slurry photoreactors, a recovery step is necessary to separate, regenerate, and reuse the photocatalyst. The efficiency of an immobilized system is less than that of the slurry photoreactor but the photocatalyst is continuously used for a longer period of time.

The disadvantages of the slurry photocatalysis include 1) difficulty and time consuming process of separation or filtration of the photocatalyst after the photocatalytic process; 2) particle aggregation and agglomeration at high photocatalyst concentration; and 3) difficulty of using the suspended photocatalyst in continuous processes (Sopyan *et al.*, 1996). To overcome these drawbacks, immobilized photocatalysts are usually recommended. Photocatalysts could be immobilized on various supports such as glasses (Sabate *et al.*, 1992; Kim *et al.*, 1995; Fernandez *et al.*, 1995; Wang *et al.*, 1998; Piscopo *et al.*, 2000; Sakthivel *et al.*, 2002; Neti *et al.*, 2010), tellerette packings (Mehrvar *et al.*, 2002), silica (Van Grieken *et al.*, 2002; Ding *et al.*, 2001; Xu *et al.*, 1999; Alemany *et al.*, 1997; López-Muñoz *et al.*, 2005; Marugán *et al.*, 2006), polymers (Kasanen *et al.*, 2009), and clays (An *et al.*, 2008).

The analysis and design of photochemical reactors have received increasing interests in chemical engineering recently. The photochemical reactors could be used to either produce and synthesize chemicals or destroy water and wastewater contaminants. The photochemical reactors are one of the least well known industrial reactors. As mentioned earlier, the main advantages of the photochemical reactors over the conventional ones are their selectivity and low reaction temperature. These advantages have become the subject of several reviews (Doede and Walker, 1955; Marcus *et al.*, 1962; Cassano *et al.*, 1967; Shirotsuka and Nishiumi, 1971; Roger and Villermaux, 1979).

3. Radiation field properties

A bundle of rays with a specific energy carrying photons is called spectral specific intensity and radiance. This parameter plays a detrimental role in radiation field inside a photoreactor. The spectral specific intensity is defined as the total amount of radiative energy passing through a unit area perpendicular to the direction of propagation, per unit solid angle about the direction, per unit frequency, and per unit time. Therefore, the spectral specific intensity unit is Einstein per square meter per stradian, per unit frequency, and per second (Cassano *et al.*, 1995):

$$I_v(x,\Omega,t,v) = \lim_{dA,d\Omega,dt,dv \to 0} \left(\frac{dE_v}{dA \cos\theta d\Omega dt dv} \right) \tag{1}$$

Another important photochemical property is the spectral incident radiation that could be calculated by integrating the spectral specific intensity over the entire photoreactor volume as follows:

$$G_v = \int_\Omega I_v d\Omega \tag{2}$$

In spherical coordinates, the spectral incident radiation could be written as follows (Cassano *et al.*, 1995):

$$G_v = \int_{\theta_1}^{\theta_2} \int_{\phi_1}^{\phi_2} I_v \sin\theta \, d\phi \, d\theta \tag{3}$$

Equation (3) is valid for the monochromatic radiation while for the polychromatic radiation, an extra integration is required as follows (Cassano *et al.*, 1995):

$$G_v = \int_{v_1}^{v_2} \int_{\theta_1}^{\theta_2} \int_{\phi_1}^{\phi_2} I_v \sin\theta \, d\phi \, d\theta \, dv \tag{4}$$

The local volumetric rate of energy absorption (LVREA), the absorbed intensity, is the product of the spectral specific intensity and the absorption coefficient. The rate of a photochemical reaction is the product of the LVREA and the quantum yield. The quantum yield indicates the number of moles of chemicals reacted per moles of photons absorbed.

4. Photon transport equation

The photon balance in a photochemical reactor can be written as follows (Ozisik, 1973; Cassano *et al.*, 1995; Alfano and Cassano, 2008):

$$\begin{bmatrix} time\,rate\,of\,change \\ of\,\Omega,v\,photons\,in \\ the\,volume \end{bmatrix} + \begin{bmatrix} net\,flux\,of\,\Omega,v\,photons \\ leaving\,the\,volume \\ across\,the\,surface\,A \end{bmatrix} = \begin{bmatrix} net\,gain\,of\,\Omega,v\,photons\,\,owning \\ to\,emission, absorption, in-scattering, \\ and\,out-scattering\,in\,the\,volume \end{bmatrix} \tag{5}$$

The right hand side of Equation (5) could be divided into two sources (emission and in-scattering) and two sink (absorption and out-scattering) terms, therefore, the photon balance equation could be written as follows (Cassano *et al.*, 1995):

$$\frac{1}{c}\frac{\partial I_{\Omega,v}}{\partial t} + \nabla \cdot \left(I_{\Omega,v}\Omega \right) = \left(W_{\Omega,v}^{em} + W_{\Omega,v}^{in-s} \right) - \left(W_{\Omega,v}^{ab} + W_{\Omega,v}^{out-s} \right) \tag{6}$$

The absorption and emission terms are useful for both homogeneous and heterogeneous photochemical reactors. The loss of photons due to the absorption could be calculated using the following expression (Cassano *et al.*, 1995):

$$W_{\Omega,v}^{ab} = K_v(x,t)I_v(x,\Omega,t) \tag{7}$$

where K_v is the absorption coefficient, which shows the fraction of the incident radiation that is absorbed by the molecule per unit length along the path of the beam. The emission term highly depends on temperature as shown in Equation (8). Photolytic and photocatalytic reactors usually operate at low temperatures, therefore, this term can be neglected for photoreactor modeling:

$$W_{\Omega,v}^{em} = K_v(x,t)I_{v,b}\big[T(x,t)\big] \tag{8}$$

The following two equations account for the gain and loss of photons due to in-scattering and out-scattering, respectively (Cassano *et al.*, 1995). In homogeneous photoreactors, these two terms (in-scattering and out-scattering) are neglected due to the absence of semiconductors:

$$W_{\Omega,v}^{s-in} = \frac{1}{4\pi} \int\limits_{\Omega'=4\pi} \int\limits_{v'=0}^{\infty} \sigma_v(x,t)p(v' \rightarrow v, \Omega' \rightarrow \Omega)I_{v'}(x,\Omega',t)dv'd\Omega' \tag{9}$$

$$W_{\Omega,v}^{s-out} = \sigma_v(x,t)I_v(x,\Omega,t) \tag{10}$$

5. Principles of photocatalysis

The photocatalytic process in a heterogeneous photoreactor takes place in the presence of a semiconductor photocatalyst, in which the whole process is divided into five stages as follows (Herrmann, 1999; Fogler, 1998; Qi *et al.*, 2011):

- Mass transfer of the organic compounds in the liquid phase to the photocatalyst surface;
- Adsorption of the pollutants onto the photoactivated semiconductor surface;
- Heterogeneous photocatalytic reaction;
- Desorption of the product(s) from the photocatalyst surface; and
- Mass transfer of the product(s) from the interface region to the bulk solution.

The most common photocatalyst is titanium dioxide (TiO_2) which catalyzes the reaction as a result of the interaction of the electrons and holes generated during the photocatalytic process. Titanium dioxide has a diverse range of applications especially in paint and coatings, plastics, sunscreens, ointments, and toothpaste. The whiteness, brightness, and opacity of titanium dioxide make the powder as a good option for a wide range of applications. Titanium dioxide exists in three different crystalline polymorphs: rutile, anatase, and brookite. TiO_2 powders could be employed in solar and UV irradiation systems (photoreactors) because this semiconductor has a high transparency to visible light, high refractive index, and low absorption coefficient.

Wide range of metal oxides and sulfides have been used as photocatalysts including ZnO (Daneshvar *et al.*, 2004; Sakthivel *et al.*, 2003; Kormann *et al.*, 1988; Khodj *et al.*, 2001; Gouvêa *et al.*, 2000; Lizama *et al.*, 2002; Kansal *et al.*, 2007; Chakrabarti and Dutta, 2004), WO_3 (Waldner *et al.*, 2007; Sayama *et al.*, 2010; Saepurahmanet *et al.*, 2010; Cao *et al.*, 2011), WS_2 (Jing and Guo, 2007), Fe_2O_3 (Chen *et al.*, 2001; Bandara *et al.*, 2001; Pal and Sharon, 1998), V_2O_5 (Akbarzadeh *et al.*, 2010; Teramura *et al.*, 2004a,b), CeO_2 (Lin and Yu, 1998; Coronado *et al.*, 2002; Ji *et al.*, 2009; Song *et al.*, 2007), CdS (Bessekhouad *et al.*, 2004; Reutergardh and Langphasuk, 1997; Tang and Huang, 1995), ZnS (Torres-Martínez *et al.*, 2001), and CuO (Lim and Kim, 2004; Sathishkumar *et al.*, 2011; Nezamzadeh-Ejheieg and Hushmandrad, 2010).

The light intensity in homogeneous and heterogeneous photoreactors determines the LVREA which is proportional to the rate of photochemical reaction. The light distribution in homogeneous photoreactors is well established. However, the heterogeneous photoreactor containing semiconductor particles makes the photoreactor modeling extremely difficult. In homogeneous photoreactors, the main solution parameter is the absorption coefficient, while in heterogeneous photoreactors, the absorption and scattering coefficients must be determined simultaneously.

6. Momentum balance and computational fluid dynamics

The momentum balance equations are applied for two flow regimes: the laminar and turbulent flow for these two single and multi-lamp photoreactors. The fluid flow in laminar regime is described by Navier-Stokes equation. For the case of the turbulent flow, different known models have been developed. Among them, the k-ε model has shown a great attraction to researchers for modeling turbulent flows. The k-ε model is a two-equation model in which fluctuating velocities and Reynolds stresses have been related to the properties of the turbulent flow itself such as k and ε. These two fluid flow properties are the turbulent kinetic energy per unit mass of the fluctuating components (k) and the turbulent dissipation rate of the kinetic energy (ε), respectively. The continuity equation and steady state momentum balances for an incompressible fluid are described by following equations (Bird *et al.*, 2002):

$$\nabla \cdot V = 0 \tag{11}$$

$$\rho V \cdot \nabla V = -\nabla P + \nabla \cdot \left(\mu + \rho \eta_T \right) \left(\nabla V + \left(\nabla V \right)^T \right) + F \tag{12}$$

In these equations, ρ, V, and P, represent the density, time-averaged turbulent velocity, and time-averaged pressure, respectively. The μ and η_T are the dynamic and kinematic turbulent viscosities, respectively. F is also the external force on the control volume.

The k-ε model depicts that the kinematic turbulent viscosity (η_T) at any point should depend only on k and ε at that point according to the following expression (Bird *et al.*, 2002):

$$\eta_T = C_\mu \frac{k^2}{\varepsilon} \tag{13}$$

where C_μ is an adjustable model constant. The turbulent kinetic energy (k) is the average kinetic energy per unit mass of eddies in the turbulent flow that is produced by the buoyant thermal and mechanically generated eddies based on the following equation (Bird *et al.*, 2002):

$$k = \frac{1}{2}\left(\overline{u'^2} + \overline{v'^2} + \overline{w'^2} \right) \tag{14}$$

Parameters u', v', and w' are the fluctuating velocities in x, y, and z directions, respectively. The steady state equations for the turbulent kinetic energy (k) and the turbulent dissipation rate (ε) are as follows (Wilkes, 2005):

$$\rho V \cdot \nabla k = \nabla \cdot \left[\left(\mu + \rho \frac{C_\mu k^2}{\sigma_k \varepsilon} \right) \nabla k \right] + \rho C_\mu \frac{k^2}{\varepsilon} \left(\nabla V + \left(\nabla V \right)^T \right)^2 - \rho \varepsilon \tag{15}$$

$$\rho V \cdot \nabla \varepsilon = \nabla \cdot \left[\left(\mu + \rho \frac{C_\mu k^2}{\sigma_\varepsilon \varepsilon} \right) \nabla \varepsilon \right] + \rho C_{\varepsilon_1} C_\mu k \left(\nabla V + \left(\nabla V \right)^T \right)^2 - \rho C_{\varepsilon_2} \frac{\varepsilon^2}{k} \tag{16}$$

All five model constants have been selected as follows such that the k-ε model gives an estimation that fits reasonably well with the experimental data (Wilkes, 2005):

$$C_\mu = 0.09; \qquad C_{\varepsilon 1} = 1.44; \qquad C_{\varepsilon 2} = 1.92; \qquad \sigma_k = 1.0; \text{ and } \qquad \sigma_\varepsilon = 1.3 \tag{17}$$

Equations (15) and (16) along with continuity and momentum Equations (11) and (12) should be solved simultaneously. Boundary conditions for the momentum balance are as follows:

Inlet of the photoreactor: The inflow velocity is specified by the ratio of the volumetric flow rate to the surface area. The k and ε are also calculated as follows:

$$k = \left(\frac{3I_T{}^2}{2}\right)\left(\overline{V}^2\right); \quad \varepsilon = C_\mu{}^{0.75}\frac{\left[\frac{3I_T{}^2}{2}\left(\overline{V}^2\right)\right]^{1.5}}{L_T}; \tag{18}$$

where I_T and L_T are the turbulent intensity scale (initial turbulence intensity) and turbulent length scale (eddy length scale). Their magnitudes could be calculated by Equations (19) and (20), respectively (Wilkes, 2005):

$$I_T = 0.16Re^{-1/8} \tag{19}$$

$$L_T = 0.07L \tag{20}$$

Outlet of the photoreactor: A normal flow is assumed so that the normal stress in the outlet is zero. Therefore, the gradient of k and ε are also calculated as follows (Wilkes, 2005):

$$\nabla k = 0 \quad ; \qquad \nabla \varepsilon = 0 \tag{21}$$

Walls of the photoreactor: No slip boundary condition could be assumed for the photoreactors and all the walls of the lamps. However, the logarithmic wall function is used for walls as a modification of the k-ε model. The boundary conditions for the k-ε model at a no-slip wall are obvious, but the near-wall behavior of the model, especially the ε-equation, is not appropriate. Therefore, the model produces poor results when integrated to the wall without modification. In fact, the integration of the k-ε model through the near-wall region and application of the no-slip conditions yield unsatisfactory results. Therefore, the logarithmic wall function is used as the boundary condition on the walls of the photoreactor and lamps. In the near-wall region, therefore, the equation is solved for the first grid node away from the wall. The logarithmic wall function for a smooth pipe, therefore, is as follows (Wilkes, 2005):

$$u_z{}^+ = 5.5 + 2.5\ln y^+$$
$$where \tag{22}$$
$$y^+ = \frac{y\sqrt{\tau_w/\rho}}{\mu/\rho} \qquad and \qquad u_z{}^+ = \frac{\overline{u_z}}{\sqrt{\tau_w/\rho}}$$

in which y^+, $u_z{}^+$, and τ_w are the dimensionless distance from the wall, the dimensionless velocity, and the wall shear stress, respectively. The y and $\overline{u_z}$ are the distance from the wall and time-averaged axial velocity, respectively.

Simultaneous solution of Equations (11), (12), (15), and (16) as well as applying boundary conditions give various flow characteristics such as velocity distribution, minimum and maximum velocities, turbulent kinetic viscosity, turbulent kinetic energy, turbulent dissipation rate distribution, and vorticity. Equations (10) to (21) are applicable to both single and multi-lamp photoreactors.

7. Case study

Annular photoreactors are the most common continuous photoreactors. These types of photoreactors contain one or more UV lamps with quartz sleeve around them. In this study, 10 different photoreactor configurations were considered for modeling purposes as listed below:

a. Single lamp photoreactor, the UV lamp is located at the center of the photoreactor;

b. Two lamp photoreactor, each of them located at 0.5R from the center line of the photoreactor;

c. Two lamp photoreactor, each of them located at 0.25R from the center line of the photoreactor;

d. Two lamp photoreactor, each of them located at 0.75R from the center line of the photoreactor;

e. Four lamp photoreactor, each of them located 0.5R from the center line of the photoreactor;

f. Four lamp photoreactor, each of them located 0.25R from the center line of the photoreactor;

g. Four lamp photoreactor, each of them located 0.75R from the center line of the photoreactor;

h. Four lamp photoreactor, two of them at 0.5R and two at 0.25R from the center line of the photoreactor;

i. Four lamp photoreactor, two of them at 0.5R and two at 0.75R from the center line of the photoreactor; and

j. Four lamp photoreactor, two of them at 0.25R and two at 0.75R from the center line of the photoreactor.

In all cases, the diameter of the quartz sleeve is assumed to be 15 mm with the photoreactor radius (R) of 200 mm. The cross sections of these photoreactors (a to j) are shown in Figures 1, 2, and 3.

The flow domains inside these photoreactors were simulated both in laminar and turbulent regimes. The inlet velocities for laminar and turbulent regimes were assumed to be 0.01 and 1 ms^{-1}, respectively. In laminar flow, the 3D Navier-Stokes equations were solved in cylindrical coordinates for single lamp and Cartesian coordinates for multilamp photoreactors. In turbulent regime, the k-ε turbulent model was used. The velocity field determination is important in the photoreactor design. The local velocity determines the residence time of the solution at a specific point. As mentioned earlier, the radiation intensity inside the photoreactor is highly non-uniform; therefore, there must be a trade-off between the residence time and the radiation intensity received at particular location.

Figures 1 and 2 depict the velocity distributions at the outlet of the photoreactors in turbulent and laminar regimes, respectively. From these two figures, three distinct regions could be considered: the region around the UV lamp(s), the region around the photoreactor wall, and the remaining parts. A lower velocity is observed around the UV lamps due to the no-slip boundary condition; therefore, a higher residence time is obtained near the UV lamps. On the other hand, around the UV lamp, a higher LVREA exist. Both higher residence time and greater radiation intensity result in a higher degradation of pollutants in water. The region near the photoreactor wall also has lower velocity and higher residence time, but the LVREA in this region is the lowest compared to those of the other regions. The light intensity was also simulated for these ten photoreactors as shown in Figure 3. In multilamp photoreactors, the light intensity of UV lamps could provide a synergetic effect depending on their location. Although closer UV lamps (in four lamp photoreactor) provide

higher light intensity in the photoreactor center, the shadowing effect of the lamps reduces the light intensity in the region near the photoreactor wall. A comparison between Figures 3e and 3f show that the photoreactor in Figure 3f performed a higher light intensity at the center, however, the shadowing effect is high, therefore, Figure 3e shows a good trade-off between the synergetic effect and the shadowing effect.
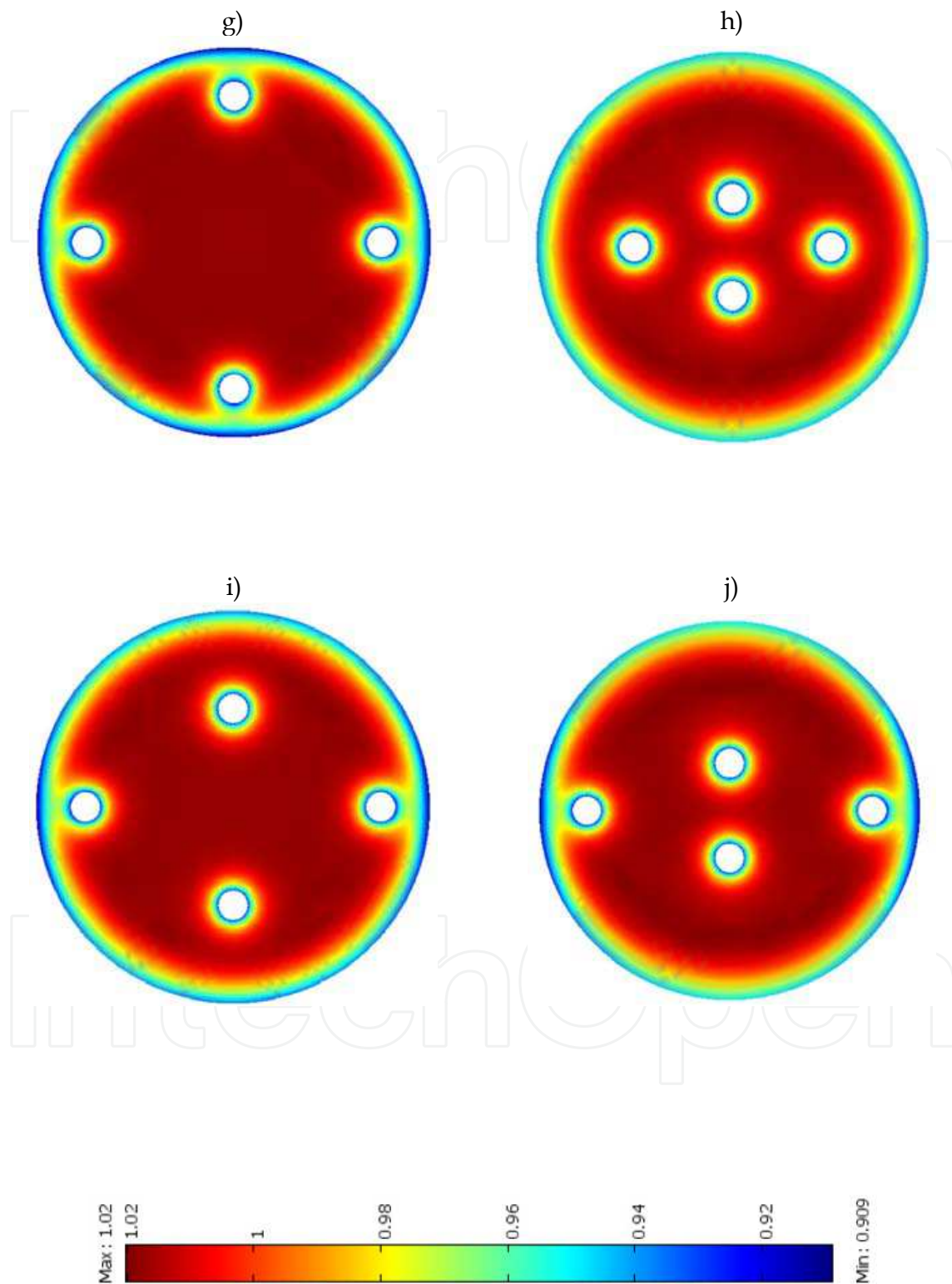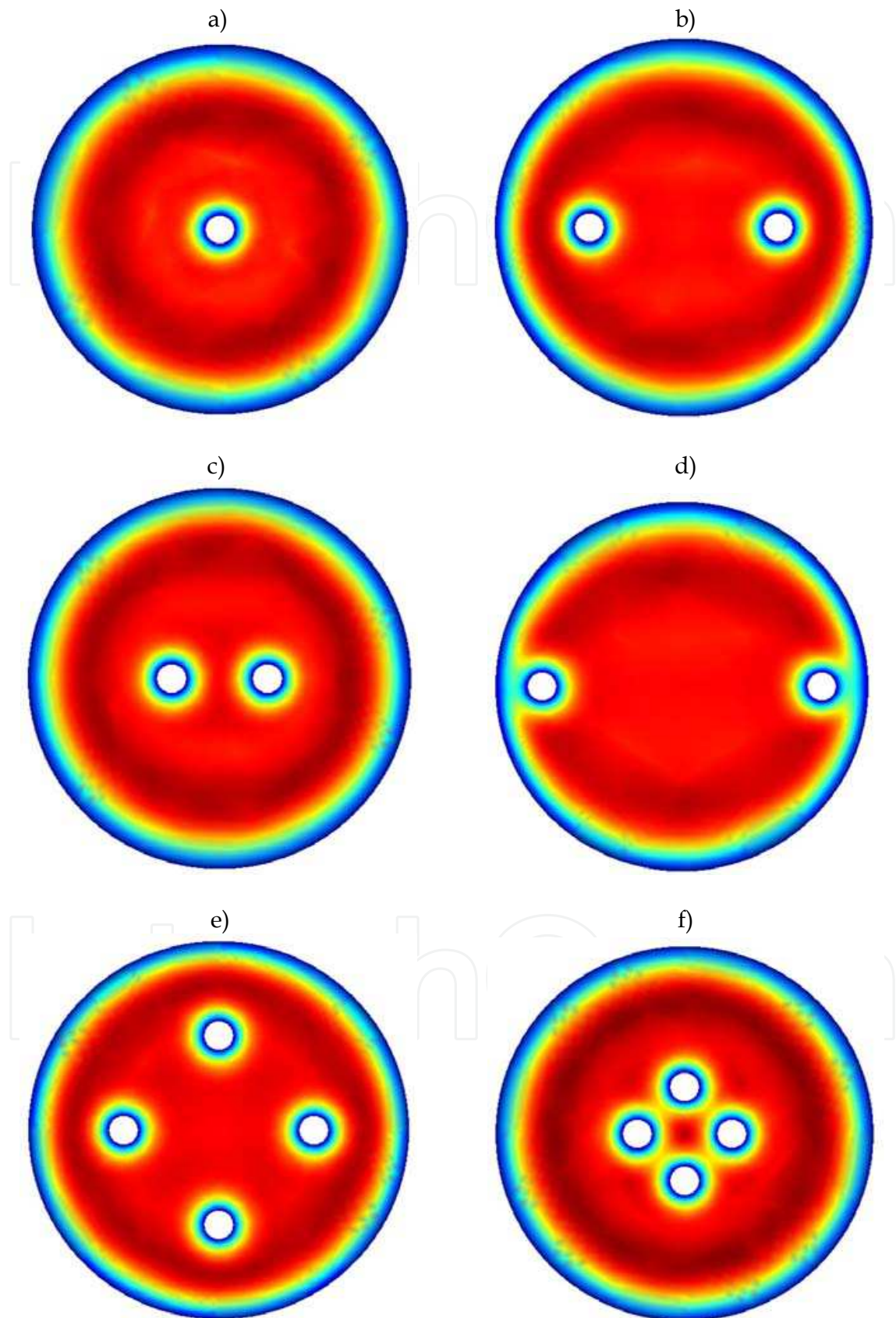
a)   b)

c)   d)

e)   f)
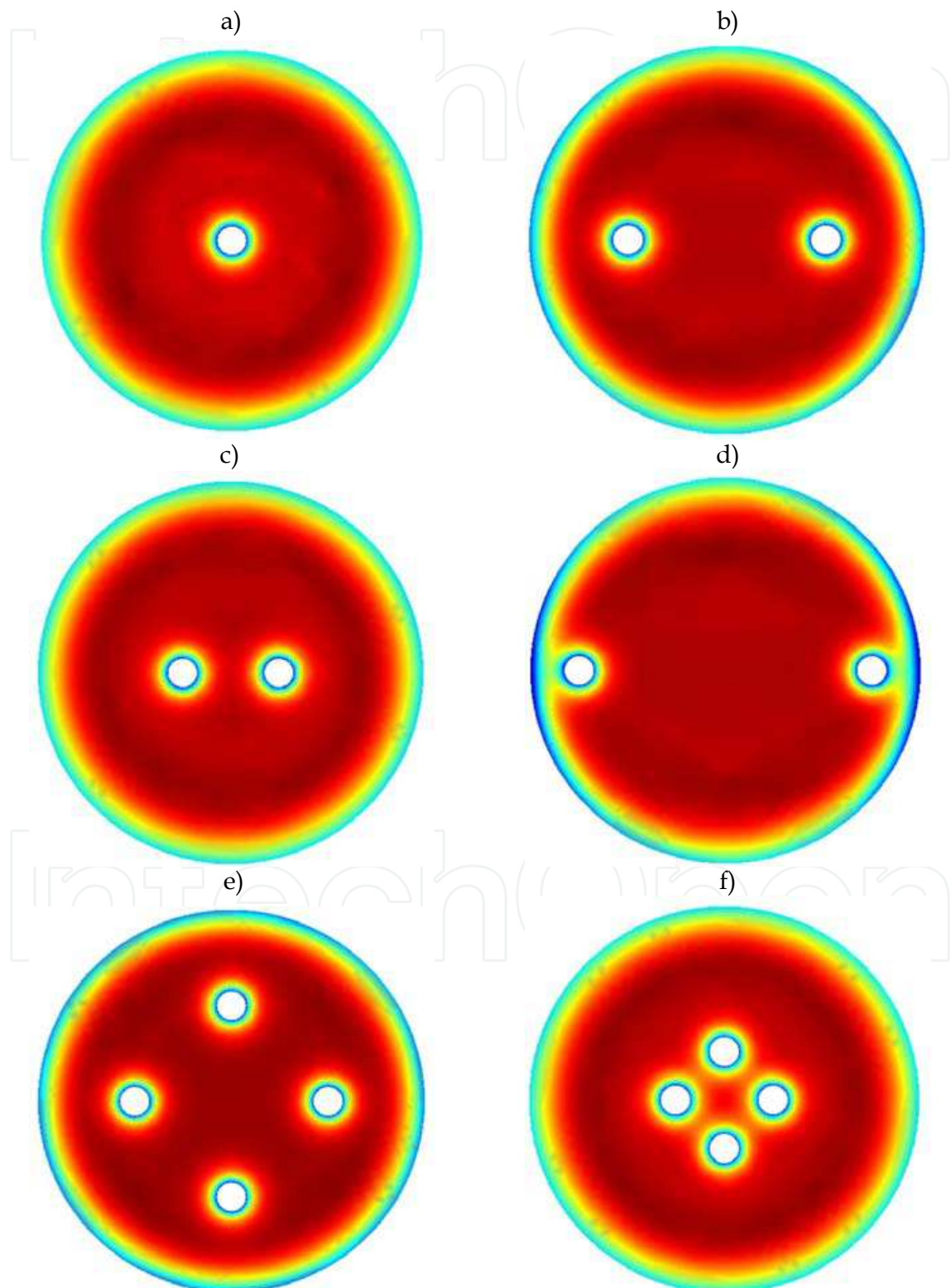
Fig. 1. Velocity distribution at the outlet of the photoreactors (turbulent regime). All geometries are defined in Section "Case study".
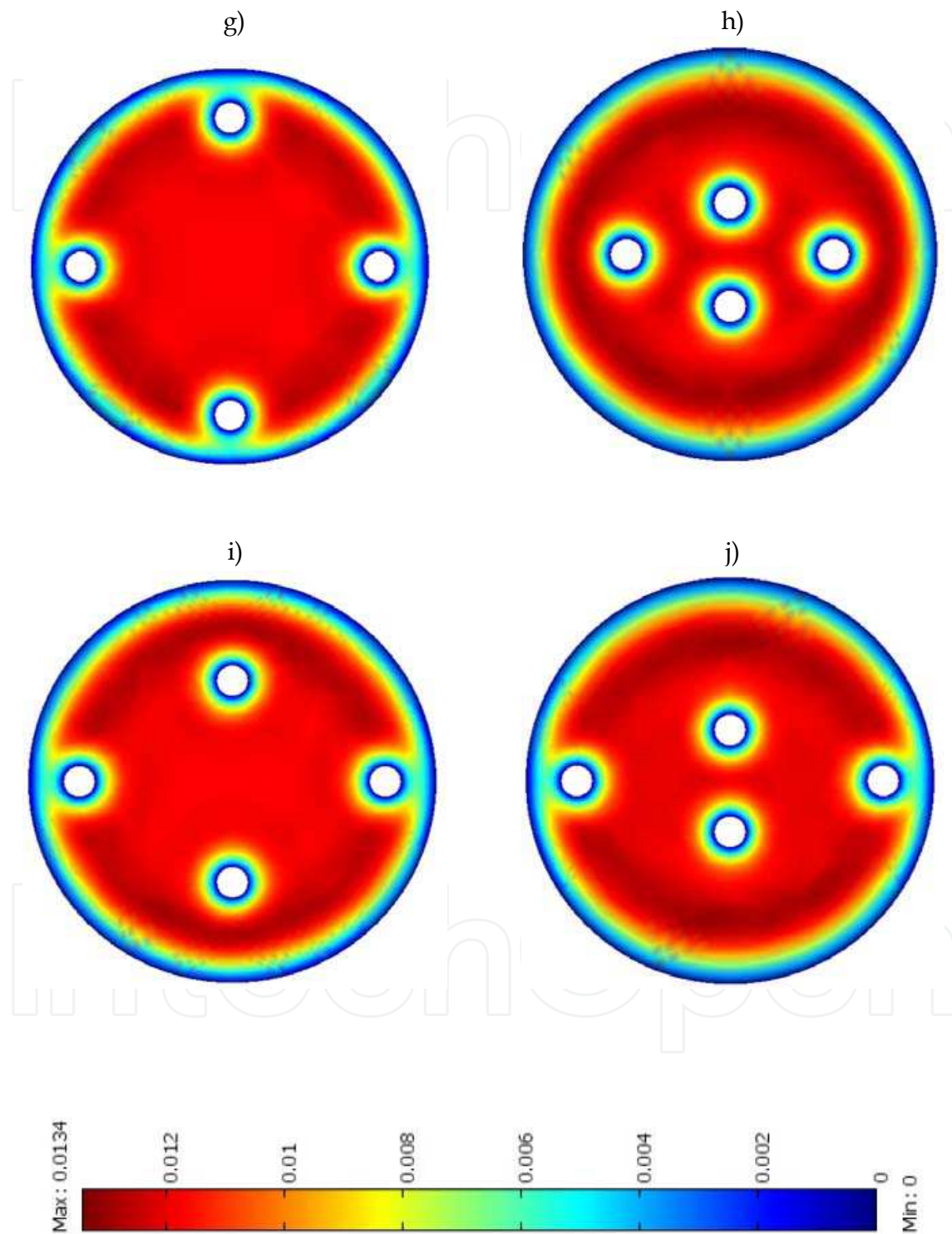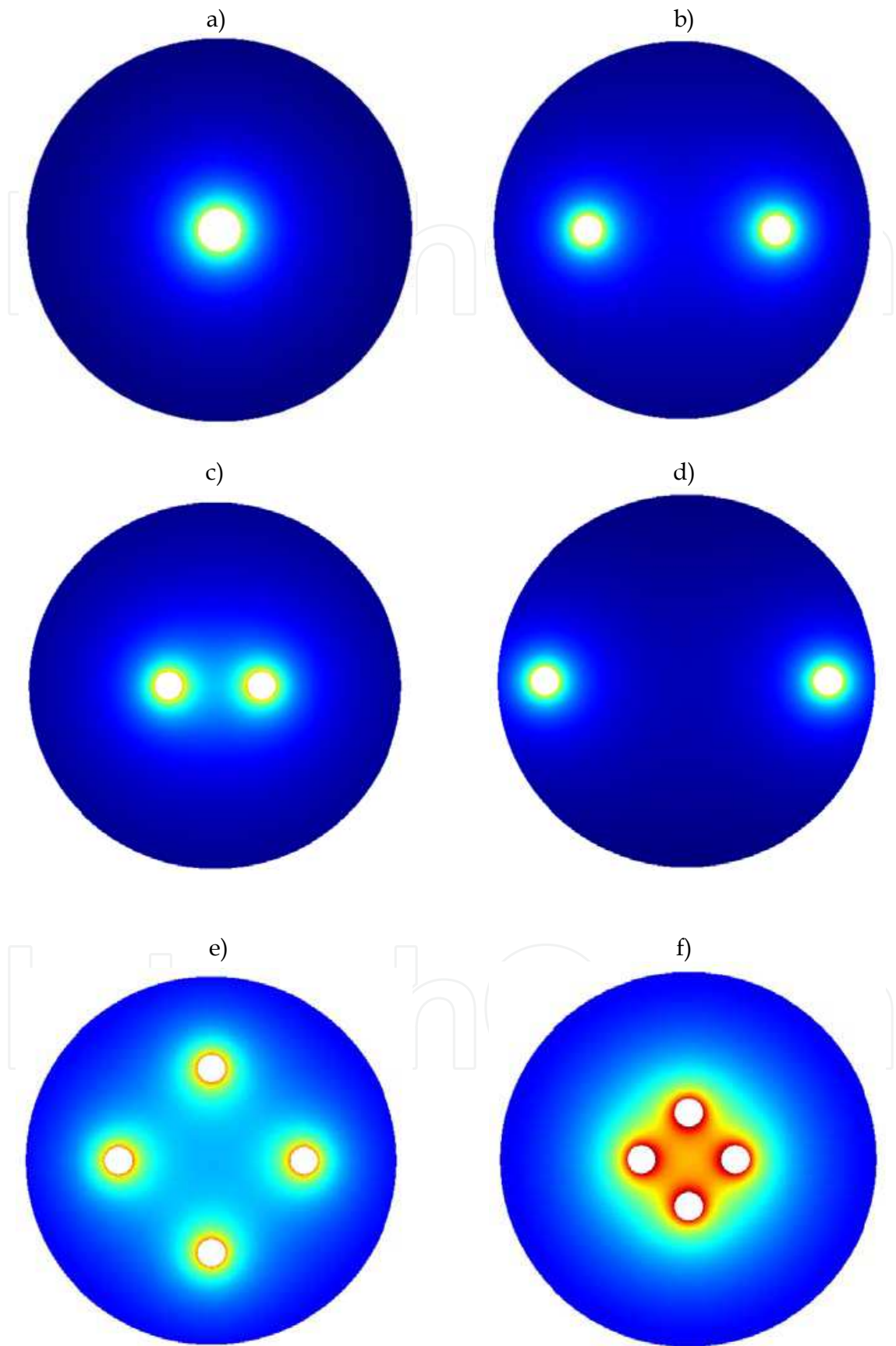
Fig. 2. Velocity distribution at the outlet of the photoreactors (laminar regime). All geometries are defined in Section "Case study".
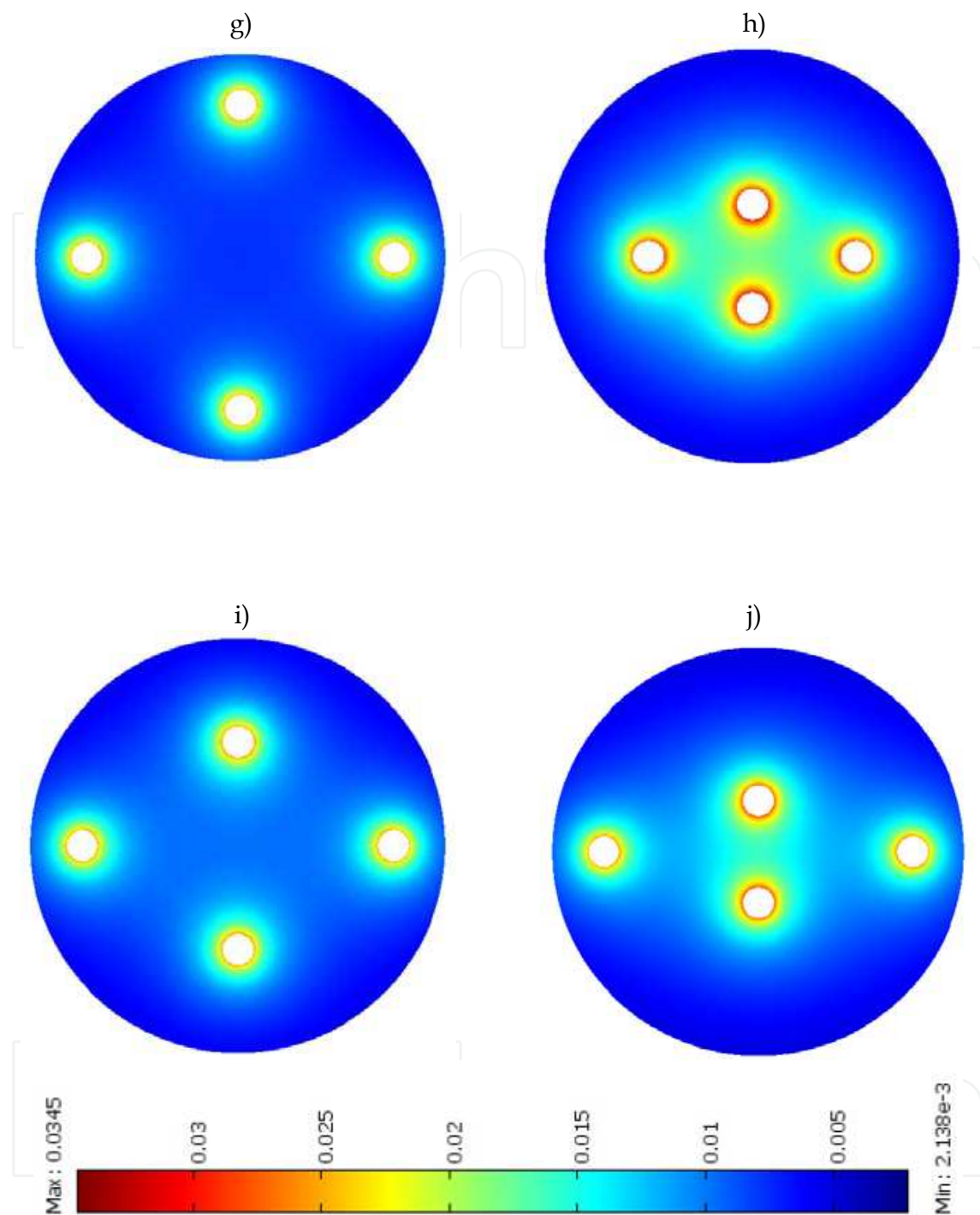
a)

b)

c)

d)

e)

f)

Fig. 3. Light intensity distribution at the outlet of the photoreactors for both laminar and turbulent regimes. All geometries are defined in Section "Case study".

8. Conclusions

The degradation and mineralization of polluted waters containing non-biodegradable compounds have become increasingly important. CFD modeling helps to design, optimize, and scale-up photochemical reactors. Velocity, light, and pollutant(s) concentration distribution would give better understanding of photoreactors operation for further

decisions. Velocity and light intensity distribution in ten different annular photoreactors were described. Velocity profiles were sketched for both laminar and turbulent flows. The effect of number and location of UV lamps was studied to find the enhancement in light distribution in multi-lamp photoreactors. Closer UV lamps performed a higher light intensity in the center of the photoreactor but the closer lamps provided a higher shadowing effect.

9. Acknowledgements

10. Nomenclature

A	area, m^2
c	light speed, $m.s^{-1}$
E_v	activation energy for frequency v, $J.mol^{-1}$
F	external force, $kg.m.s^{-2}$
G_v	incident radiation, $Einstein.s^{-1}.m^{-2}$
I_v	Specific intensity for frequency v, $Einstein.s^{-1}.m^{-2}.sr^{-1}$
I_T	turbulent intensity scale, dimensionless
k	turbulent kinetic energy, $m^2.s^{-2}$
K	reaction rate constant, $m^3.mol.^{-1}s^{-1}$
L_T	turbulent length scale, m
L	equivalent diameter of the photoreactor, m
P	time-averaged pressure, pa
R	photoreactor radius, m
t	time, s
T	temperature, K
u'	fluctuating velocity in x direction, $m.s^{-1}$
u_z^+	dimensionless velocity
V	time-averaged turbulent velocity, $m.s^{-1}$
v'	fluctuating velocity in y direction, $m.s^{-1}$
w'	fluctuating velocity in z direction, $m.s^{-1}$
W	gain or loss of energy, $Einstein.s^{-1}.m^{-3}.sr^{-1}$
x	position vector, m
y	position on y-axis (distance from the wall), m
y^+	dimensionless distance from the wall

Greek letters

ε	turbulent dissipation rate, $m^2.s^{-3}$
η_T	turbulent kinematic viscosity, $m^2.s^{-1}$
θ	spherical coordinate, rad
μ	dynamic viscosity, $kg.m^{-1}.s^{-1}$
v	frequency, s^{-1}
ρ	density, $kg.m^{-3}$
σ	volumetric scattering coefficient, m^{-1}
τ_w	wall shear stress, $kg.m^{-1}.s^{-2}$

ϕ spherical coordinate, rad
Ω unit vector in the direction of propagation, dimensionless

11. References

Akbarzadeh, R.; Umbarkar, S.B.; Sonawane, R.S.; Takle, S. & Dongare, M.K. (2010) Vanadia-titania thin films for photocatalytic degradation of formaldehyde in sunlight. *Appl. Catal. A: General*, Vol. 374 No. 1-2 pp. 103-109.

Akehata, T. & Shirai, T. (1972) Effect of light-source characteristics on the performance of circular annular photochemical reactor. *J. Chem. Eng. Japan* Vol. 5 pp.385-391.

Alemany, L.J.; Bañares, M.A.; Pardo, E.; Martin, F.; Galán-Fereres, M. & Blasco, J.M. (1997) Photodegradation of phenol in water using silica-supported titania catalysts. *Appl. Catal. B: Environ.*, Vol. 13, No. 3-4, pp. 289-297.

Alfano, O.M.; Romero, R.L. & Cassano, A.E. (1986a) Radiation field modelling in photoreactors-II. Heterogeneous media. *Chem. Eng. Sci.*, Vol. 41 No. 5 pp. 1137-1153.

Alfano, O.M.; Romero, R.L. & Cassano, A.E. (1986b) Radiation field modelling in photoreactors-I. Homogeneous media. *Chem. Eng. Sci.*, Vol. 41 No. 5 pp. 421-444.

Alfano, O.M. & Cassano, A.E. (2008) Photoreactor modeling: applications to advanced oxidation processes. *Int. J. Chem. Reactor Eng.*, Vol. 6, P2, pp.1-18.

Alfano, O.M. & Cassano, A.E. (2009) Scalling-up of photoreactors. Applications to advanced oxidation process. *Adv. Chem. Eng.*, Vol. 36 pp. 229-287.

An, T.; Chen, J.; Li, G.; Ding, X.; Sheng, G.; Fu, J.; Mai, B. & O'Shea, K.E. (2008) Characterization and the photocatalytic activity of TiO_2 immobilized hydrophobic montmorillonite photocatalysts. Degradation o decabromodiphenyl ether (BDE 209). *Catal. Today* Vol. 139 No. 1-2, pp. 69-76.

Bandara, J.; Mielczarski, J.A.; Lopez, A. & Kiwi, J. (2001) Sensitized degradation of chlorophenols on iron oxides induced by visible light comparison with titanium oxide. *Appl. Catal. B: Environ*, Vol. 34 No. 4 pp. 321-333.

Bessekhouad, Y.; Robert, D. & Weber, J.V. (2004) Bi_2S_3/TiO_2 and CdS/TiO_2 heterojunctions as an available configuration for photocatalytic degradation of organic pollutant. *J. Photochem. Photobiol. A: Chemistry*, Vol. 163 No. 3 pp. 569-580.

Bird, R.B.; Steward, W.E. & Lightfood, E.N. Transport Phenomena, 2nd ed. John Wiley & Sons, Inc.: NY, 2002

Cao, J.; Luo, B.; Lin, H. & Chen, S. (2011) Photocatalytic activity of novel $AgBr/WO_3$ composite photocatalyst under visible light irradiation for methyl orange degradation. *J. Hazard.s Mater.*, Vol. 190 No. 1-3 pp. 700-706.

Cassano, A.E. & Smith, J.M. (1966) Photochlorination in a tubular reactor. *AIChE J.*, Vol. 12 pp. 1124-1133.

Cassano, A.E. & Smith, j.M. (1967) Photochlorination of propane. *AIChE J.*, Vol. 13, pp. 915-925.

Cassano, A.E.; Silverston, P.L. & Smith, J.M. (1967) Photochemical reaction engineering. *Ind. Eng. Chem.*, Vol. 59, pp. 18-38.

Cassano, A. E.; Matsuura, T. & Smith, J.M. (1968) Batch recycle reactor for slow photochemical reactions. *Ind. Eng. Chem. Fundam.*, Vol. 7 pp. 655-660.

Cassano, A.E.; Martín, C.A.; Brandi, R.J. & Alfano, O.M. (1995) Photoreactor analysis and design: Fundamentals and applications. *Ind. Eng. Chem. Res.*, Vol. 34, No. 7, pp. 2155-2201.

Chakrabarti, S. & Dutta, B.K. (2004) Photocatalytic degradation of model textile dyes in wastewater using ZnO as semiconductor catalyst. *J. Hazard. Mater.*, Vol. 112 No. 3 pp. 269-278

Chen, F.; Xie, Y.; Zhao, J. & Lu, G. (2001) Photocatalytic degradation of dyes on a magnetically separated photocatalyst under visible and UV irradiation. *Chemosphere*, Vol. 44 No. 5 pp. 1159-1168.

Coronado, J.M.; Javier Maira, A.; Martínez-Arias, A.; Conesa, J.C. & Soria, J. (2002) EPR study of the radicals formed upon UV irradiation of ceria-based photocatalysts. *J. Photochem. Photobiol. A: Chemistry*, Vol. 150 No. 1-3 pp. 213-221.

Daneshvar, N.; Salari, D. & Khataee, A.R. (2004) Photocatalytic degradation of azo dye acid red 14 in water on ZnO as an alternative catalyst to TiO$_2$ *J. Photochem. Photobiol. A: Chemistry*, Vol. 162; No. 2-3; pp.317-322.

Denny, F.; Scott, J.; Pareek, V.; Peng, G.-D. & Amal, R. (2010) Computational fluid dynamics modelling and optimal configuring of a channeled optical fibre photoreactor. *Chem. Eng. Sci.*, Vol. 65 No. 17 pp. 5029-5040.

Ding, Z.; Hu, X.; Yue, P.L.; Lu, G.Q. & Greenfield, P.F. (2001) Synthesis of anatase TiO$_2$ supported on porous solids by chemical vapor deposition. *Catal. Today*, Vol. 68, No.: 1-3; pp. 173-182.

Doede, C.M. & Walker, C.A. (1955). Photochemical engineering. *Chemical Engineering*, pp. 159-178.

Dolan, W.J.; Dimon, C.A. & Dranoff, J.S. (1965) Dimensional analysis in photochemical reactor design. *AIChE J.*, Vol. 11 pp. 1000-1005.

Duran, J.E.; Taghipour, F. & Mohseni, M. (2011a) Evaluation of model parameters for simulating TiO$_2$ coated UV reactors. *Water Sci. Technol.*, Vol. 63 No. 7 pp. 1366-1372.

Duran, J.E.; Mohseni, M. & Taghipour, F. (2011b) Design improvement of immobilized photocatalytic reactors using a CFD-Taguchi combined method. *Ind. Eng. Chem. Res.*, Vol. 50 No. 2 pp. 824-831.

Duran, J.E.; Taghipour, F. & Mohseni, M. (2010) Irradiance modeling in annular photoreactors using the finite-volume method. *J. Photochem. Photobiol. A: Chemistry*, Vol. 215 No. 1 pp. 81-89.

Dworkin, D. & Dranoff, J.S. (1978) Free radical transport in a photochemical reactor. *AIChE J.*, Vol. 24 pp. 1134-1137.

Elyasi, S. & Taghipour, F. (2006) Simulation of UV photoreactor for water disinfection in Eulerian Framework. *Chem. Eng. Sci.*, Vol. 61 No. 14 pp. 4741-4749.

Elyasi, S. & Taghipour, F. (2010) Simulation of UV photoreactor for degradation of chemical contaminants: Model development and evaluation. *Environ. Sci. Technol.*, Vol. 44 No. 6 pp. 2056-2063.

Fernandez, A.; Lassaletta, G.; Jimenez, V.Z.; Justo, A.; Gonzalez-Elipe, A.R.; Herrmann, J.M.; Tahiri, H. & Ait-Ichou, Y. (1995) Preparation and characterization of TiO$_2$ photocatalysts supported on various rigid supports (glass, quartz and stainless steel). Comparative studies of photocatalytic activity in water purification. *Appl. Catal. B: Environ.*, Vol. 7 No. 1-2 pp. 49-63.

Fogler, H.S. Elements of Chemical Reaction Engineering, third ed., Prentic Hall PTR, New Jersey, 1998.

Gaertner, R.F. & Kent, J.A. (1958) Conversion in a continuous photochemical reactor. *Ind. Eng. Chem. Res.*, Vol. 50 No. 9, pp. 1223-1226.

Gouvêa, C.A.K.; Wypych, F.; Moraes, S.G.; Durán, N.; Nagata, N. & Peralta-Zamora, P. (2000) Semiconductor-assisted photocatalytic degradation of reactive dyes in aqueous solution. *Chemosphere*, Vol. 40 No. 4 pp. 433-440.

Harada, J.; Akehata, T. & Shirai, T. (1971) Light intensity distribution in an elliptical photoreactor. *Kagaku Kogaku,* Vol. 35 pp. 233-239.

Harris, P.R. & Dranoff, J.S. (1965) A study of perfectly mixed photochemical reactors. *AIChE J.,* Vol. 11 pp. 497-502.

Herrmann, J.-M. (1999) Heterogeneous photocatalysis: Fundamentals and applications to the removal of various types of aqueous pollutants. *Catal. Today*, Vol. 53 No. 1 pp. 115-129.

Jacob, S.M. & Dranoff, J.S. (1966) Radial scale-up of perfectly mixed photochemical reactors. *Chem. Eng. Prog. Symp. Ser.*, Vol. 62 pp.47-55.

Jacob, S.M. & Dranoff, J.S. (1968) Design and analysis of perfectly mixed photochemical reactors. *Chem. Eng. Prog. Sym. Ser.*, Vol. 64 pp. 54-63.

Jacob, S.M. & Dranoff, J.S. (1969) Light intensity profiles in an elliptical photoreactor. *AIChE J.,* Vol. 15 pp. 141-144.

Jacob, S.M. & Dranoff, J.S. (1970) Light intensity profiles in a perfectly mixed photoreactor. *AIChE J.,* Vol. 16 pp. 359-363.

Jain, R.L.; Graessley, W.W. & Dranoff, J.S. (1971) Design and analysis of a photoreactor for styrene polymerization. *Ind. Eng. Chem. Prod. Res. Develop.*, Vol. 10 pp. 293-298.

Ji, P.; Zhang, J.; Chen, F. & Anpo, M. (2009) Study of adsorption and degradation of acid orange 7 on the surface of CeO_2 under visible light irradiation. *Appl. Catal. B: Environment.*, Vol. 85 No. 3-4 pp. 148-154.

Jing, D. & Guo, L. (2007) WS_2 sensitized mesoporous TiO_2 for efficient photocatalytic hydrogen production from water under visible light irradiation. *Catal. Commun.*, Vol. 8 No. 5 pp. 795-799.

Kansal, S.K.; Singh, M. & Sud, D. (2007) Studies on photodegradation of two commercial dyes in aqueous phase using different photocatalysts. *J. Hazard. Mater.*, Vol. 141 No. 3 pp. 581-590.

Kasanen, J.; Suvanto, M. & Pakkanen, T.T. (2009) Self-cleaning, titanium dioxide based, multilayer coating fabricated on polymer and glass surfaces. *J. Appl. Polym. Sci.*, Vol. 111 No. 5 pp. 2597-2606.

Kim, D.H.; Anderson, M.A. & Zeitner, W.A. (1995) Effects of firing temperature on photocatalytic and photoelectrocatalytic properties of TiO_2. *J. Environ. Eng.*, Vol. 121 No. 8 pp. 590-594.

Khodja, A.A.; Sehili, T.; Pilichowski, J.-F. & Boule, P. (2001) Photocatalytic degradation of 2-phenylphenol on TiO_2 and ZnO in aqueous suspensions. *J. Photochem. Photobiol. A: Chemistry*, Vol. 141 No. 2-3 pp. 231-239.

Kormann, C.; Bahnemann, D.W. & Hoffmann, M.R. (1988) Photocatalytic production of H_2O_2 and organic peroxides in aqueous suspensions of TiO_2, ZnO, and desert sand. *Environ. Sci. Technol.*, Vol. 22 No. 7 pp. 798-806.

Lim, T.H. & Kim (2004), S.D. Trichloroethylene degradation by photocatalysis in annular flow and annulus fluidized bed photoreactors. *Chemosphere*, Vol. 54 No. 3 pp. 305-312.

Lin, J. & Yu, J.C. (1998) An investigation on photocatalytic activities of mixed TiO_2-rare earth oxides for the oxidation of acetone in air. *J. Photochem. Photobiol. A: Chemistry*, Vol. 116 No. 1 pp. 63-67.

Lizama, C.; Freer, J.; Baeza, J. & Mansilla, H.D. (2002) Optimized photodegradation of reactive blue 19 on TiO_2 and ZnO suspensions. *Catalysis Today,* Vol. 76 No. 2-4 pp. 235-246.

López-Muñoz, M.-J.; Grieken, R.V.; Aguado, J. & Marugán, J. (2005) Role of the support on the activity of silica-supported TiO_2 photocatalysts: structures of the TiO_2/SBA-15 photocatalysis. *Catal. Today*, Vol. 101, pp. 307-314.

Magelli, F. & Santarelli, F. (1978) The modelling of batch photoreactors. *Chem. Eng. Sci.*, Vol. 33 pp. 611-614.

Marcus, R.J.; Kent, J.A. & Schenck, G.O. (1962) Industrial photochemistry. *Ind. Eng. Chem.*, Vol. 54, pp. 20-28

Marugán, J.; Hufschmidt, D.; López-Muñoz, M.-J.; Selzer, V. & Bahnemass, D. (2006) Photonic efficiency for methanol photooxidation and hydroxyl radical generation on silica-supported TiO_2 photocatalysts. *Appl. Catal. B: Environ*, Vol: 62, No.: 3-4, pp. 201-207.

Matsuura, T.; Cassano, A.E. & Smith, J.M. (1969) Acetone photolysis: kinetic studies in a flow reactor. *AIChE J.,* Vol. 15 pp. 495-501.

Matsuura, T. & Smith, J.M. (1970a) Light distribution in cylindrical photoreactors. *AIChE J.*, Vol. 16 pp. 321-324.

Matsuura, R. & Smith, J.M. (1970b) Kinetics of photocomposition of dodecyl benzene sulfonate. *Ind. Eng. Chem. Fund.*, Vol. 9 pp. 252-260.

Matsuura, R. & Smith, J.M. (1970c) Photodecomposition kinetics of formic acid in aqueous solutions. *AIChE J.*, Vol. 16 pp.1064-1071.

Matsuura, R. & Smith, J.M. (1971) Photodecomposition kinetics of formic acid in aqueous solutions. *Ind. Eng. Chem. Fundam.*, Vol. 10, pp. 316-318.

Mehrvar, M.; Anderson, W.A. & Moo-Young, M. (2002) Preliminary analysis of a tellerette packed-bed photocatalytic reactor, *Adv. Environ. Res.* Vol. 6 No. 4, pp. 411–418.

Mohajerani, M.; Mehrvar, M. & Ein-Mozaffari, F. (2011) Photoreactor design and CFD modelling of a UV/H_2O_2 process for distillery wastewater treatment. *Can. J. Chem. Eng.* (in press).

Mohajerani, M.; Mehrvar, M. & Ein-Mozaffari, F. (2010) CFD modeling of metronidazole degradation in water by the UV/H_2O_2 process in single and multilamp photoreactors. *Ind. Eng. Chem. Res.*, Vol. 49 No. 11 pp. 5367-5382.

Mohseni, M. & Taghipour, F. (2004) Experimental and CFD analysis of photocatalytic gas phase vinyl chloride (VC) oxidation. *Chem. Eng. Sci.*, Vol. 59 No. 7 pp. 1601-1609.

Neti, N.R.; Parmar, G.R.; Bakardjieva, S. & Subrt, J. (2010) Thick film titania on glass supports for vapour phase photocatalytic degradation of toluene, acetone, and ethanol. *Chem. Eng. J.*, Vol. 163 No. 3 pp. 219-229.

Nezamzadeh-Ejhieh, A. & Hushmandrad, S. (2010) Solar photodecolorization of methylene blue by CuO/X zeolite as a heterogeneous catalyst. *Appl. Catal. A: General,* Vol. 388 No. 1-2 pp. 149-159.

Ozisik, M.N. (1973) Radiative transfer and interactions with conduction and convection, Wiley, New York

Pal, B. & Sharon, M. (1998) Photocatalytic degradation of salicylic acid by colloidal Fe_2O_3 particles. *J. Chem. Technol. Biotechnol.*, Vol. 73 No. 3 pp. 269-273.

Pasquali, G. & Santarelli, F. (1978) Radiant energy transfer in batch photoreacting media. *Chem. Eng. Commun.*, Vol.2 pp. 271-274.

Piscopo, A.; Robert, D.; Marzolin, C. & Weber, J.V. (2000) TiO_2 supported on glass fiber for the photocatalytic degradation of benzamide. *J. Mater. Sci. Lett.*, Vol. 19 No. 8 pp. 683-684.

Qi, N.; Zhang, H.; Jin, B. & Zhang, K. (2011) CFD modelling of hydrodynamics and degradation kinetics in an annular slurry photocatalytic reactor for wastewater treatment. *Chem. Eng. J.*, (in press).

Reutergardh, L.B. & Langphasuk, M. (1997) Photocatalytic decolourization of reactive azo dye: A comparison between TiO_2 and CdS photocatalysis. *Chemosphere*, Vol. 35 No. 3 pp. 585-596.

Roger, M. & Villermaux, J. (1983) Modelling of light absorption in photoreactors. Part II. Density profile and efficiency of light absorption in a cylindrical reactor. Experimental comparison with complex kinetics. *Chem. Eng. Sci.*, Vol. 38 pp. 1593-1605.

Roger, M. & Villermaux, J. (1979) Modelling of light absorption in photoreactors. Part I. General formulation based on the laws of photometry. *Chem. Eng. J.*, Vol. 17, pp. 219-226.

Sabate, J.; Anderson, M.A.; Aguado, M.A.; Giménez, J.; Cervera-March, S. & Hill Jr., C.G. (1992) Comparison of TiO_2 powder suspensions and TiO_2 powder suspensions and TiO_2 ceramic membrans supported on glass as photocatalytic systems in the reduction of chromium. *J. Mol. Catal.*, Vol. 71 No. 1 pp. 57-68.

Saepurahman, Abdullah, M.A. & Chong, F.K. (2010) Preparation and characterization of tungsten-loaded titanium dioxide photocatalyst for enhanced dye degradation. *J. Hazard. Mater.*, Vol. 176 No. 1-3 pp. 451-458.

Sakthivel, S.; Shankar, M.V.; Palanichamy, M.; Arabindoo, B. & Murugesan, V. (2002) Photocatalytic decomposition of leather dye. Comparative study of TiO_2 supported on alumina and glass beads. *J. Photochem. Photobiol. A: Chemistry*, Vol. 148 No. 1-3 pp. 153-159.

Sakthivel, S.; Neppolian, B.; Shankar, M.V.; Arabindoo, B.; Palanichamy, M. & Murugesan, V. (2003) Solar photocatalytic degradation of azo dye: Comparison of photocatalytic efficiency of ZnO and TiO_2. *Sol. Energy Mater. Sol. Cells*, Vol. 77 No. 1, pp.65-82.

Santarelli, F. & Smith, J.M. (1974) Rate of photochlorination of liquid n-heptane. *Chem. Eng. Commun.*, Vol. 1, pp. 297-302.

Sathishkumar, P.; Sweena, R. & Wu, J.J. (2011) Anandan, S. Synthesis of CuO-ZnO nanophotocatalyst for visible light assisted degradation of a textile dye in aqueous solution. *Chem. Eng. J.*, Vol. 171 No. 1 pp. 136-14.

Sayama, K.; Hayashi, H.; Arai, T.; Yanagida, M.; Gunji, T. & Sugihara, H. (2010) Highly active WO_3 semiconductor photocatalyst prepared from amorphous peroxotungstic acid for the degradation of various organic compounds. *Appl. Catal. B: Environ.*, Vol. 94 No. 1-2 pp.150-157.

Schechter, R.S. & Wissler, E.H. (1960) Photochemical reactions in an isothermal laminar-flow chemical reactor. *Appl. Sci. Res.*, Vol. 9 No. 1, pp. 334-344

Shirotsuka, T. & Nishiumi, H. (1971) Theoretical basis for making an apparatus for photochemical reactions. *Kagaku Kogaku*, Vol. 35, pp. 1329-1338.

Song, S.; Xu, L.; He, Z.; Chen, J.; Xiao, X. & Yan, B. (2007) Mechanism of the photocatalytic degradation of C.I. reactive black 5 at pH 12.0 using $SrTiO_3/CeO_2$ as the catalyst. *Environ. Sci. Technol.*, Vol. 41 No. 16 pp. 5846-5853.

Sopyan, I.; Watanabe, M.; Murasawa, S.; Hashimoto, K. & Fujishima, A. (1996) An efficient TiO_2 thin-film photocatalyst: photocatalytic properties in gas-phase acetaldehyde degradation. *J. Photochem. Photobiol.*, Vol. 98 No. 1-2. pp. 79-86.

Taghiour, F. & Mohseni, M. (2005) CFD simulation of UV photocatalytic reactors for air treatment. *AIChE J.*, Vol. 51 No. 11 pp. 3039-3047.

Tang, W.Z. & Huang, C.P. (1995) Photocatalyzed oxidation pathways of 2,4-dichlorophenol by CdS in basic and acidic aqueous solutions. *Water Res.*, Vol. 29 No. 2 pp. 745-756.

Teramura, K.; Tanaka, T.; Kani, M.; Hosokawa, T. & Funabiki, T. (2004a) Selective photo-oxidation of neat cyclohexane in the liquid phase over V_2O_5/Al2O3. *J. Mol. Catal. A: Chem.*, Vol. 208 No. 1-2 pp. 299-305.

Teramura, K.; Tanaka, T.; Hosokawa, T.; Ohuchi, T.; Kani, M. & Funabiki, T. (2004b) Selective photo-oxidation of various hydrocarbons in the liquid phase over V_2O_5/Al_2O_3. *Catal. Today*, Vol. 96 No. 4 pp. 205-209.

Torres-Martínez, C.L.; Kho, R.; Mian, O.I. & Mehra, R.K. (2001) Efficient photocatalytic degradation of environmental pollutants with mass-produced ZnS nanocrystals. *J. Colloid Interface Sci.*, Vol. 240 No. 2 pp. 525-532.

Van Grieken, R.; Aguado, J.; López-Muoz, M.J. & Marugán, J. (2002) Synthesis of size-controlled silica-supported TiO_2 photocatalysts. *J. Photochem. Photobiol. A: Chemistry*, Vol. 148 No. 1-3, pp. 315-322.

Vincent, G.; Schaer, E.; Marquaire, P.-M. & Zahraa, O. (2011) CFD modelling of an annular reactor, application to the photocatalytic degradation of acetone. *Process Saf. Environ. Prot.*, Vol. 89 No. 1 pp. 35-40.

Waldner, G.; Brüger, A.; Gaikwad, N.S. & Neumann-Spallart, M. (2007) WO_3 thin films for photoelectrochemical purification of water. *Chemosphere*, Vol. 67 No. 4 pp. 779-784.

Wang, K.-H.; Tsai, H.-H. & Hsieg, Y.-H. (1998) The kinetics of photocatalytic degradation of trichloroethylene in gas phase over TiO_2 supported on glass beads. *Appl. Catal. B: Environ.*, Vol. 17 No. 1-2 pp. 25-36.

Wilkes, J.O. Fluid mechanics for chemical engineers with microfluidics and CFD, 2nd ed. Prentice Hall: NJ, 2005.

Williams, J.A. & Ragonese, F.P. (1970) Asymptotic solutions and limits of transport equations for tubular flow photoreactors. *Chem. Eng. Sci.*, Vol. 25 pp. 1751-1759.

Williams, J.A. (1978) The radial light intensity profile in cylindrical photoreactors. *AIChE J.*, Vol. 24 pp. 335-338.

Xu, Y.; Zheng, W. & Liu, W. (1999) Enhanced photocatalytic activity of supportedTiO2: Dispersing effect of SiO_2. *J. Photochem. Photobiol. A: Chemistry*, Vol. 122, No.: 1, pp. 57-60.
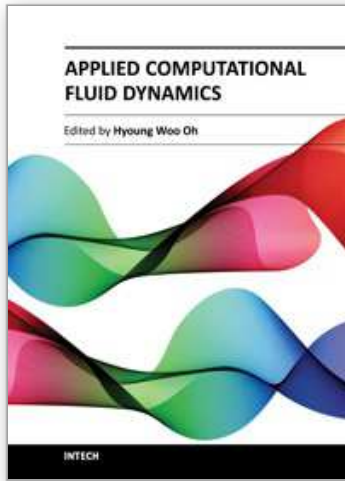
Applied Computational Fluid Dynamics

Edited by Prof. Hyoung Woo Oh

This book is served as a reference text to meet the needs of advanced scientists and research engineers who seek for their own computational fluid dynamics (CFD) skills to solve a variety of fluid flow problems. Key Features: - Flow Modeling in Sedimentation Tank, - Greenhouse Environment, - Hypersonic Aerodynamics, - Cooling Systems Design, - Photochemical Reaction Engineering, - Atmospheric Reentry Problem, - Fluid-Structure Interaction (FSI), - Atomization, - Hydraulic Component Design, - Air Conditioning System, - Industrial Applications of CFD

How to reference

In order to correctly reference this scholarly work, feel free to copy and paste the following:

INTECH
open science | open minds